DOI: https://doi.org/10.52651/sam.a.2021.1.19-24

EXPERIMENTAL DETERMINATION OF CONTINUOUS COOLING TRANSFORMATION DIAGRAM FOR HIGH STRENGTH STEEL X153CRMOV12

Michal KRBAŤA, Róbert CÍGER

Abstract: The article is a continuation of the article ‚DILATOMETRIC ANALYSIS OF COOLING CURVES FOR HIGH STRENGTH STEEL X153CrMoV12", which deals with the phase transformations of tool steel X153CrMoV12. The experimental data obtained was used to evaluate the resulting CCT diagram, which consists of seven dilation curves. All experimental samples from dilatometric analyses were then subjected to microstructural analysis and hardness measurements to characterize the microstructure and hardness for each heat treatment mode tested. AFM microscopy was also used to study the carbides present in steels and their size and shape for all selected cooling modes.

Keywords: Dilatometry; Tool steel; Cooling rate; Martensite; CCT diagram.

1 INTRODUCTION

In practical situations, Continuous Cooling Transform (CCT) diagram play an important role in the development of high-strength advanced steels. The CCT diagrams allow accurate predictions of the microstructures compositions that may arise in the real processing of these steels. They are generally used to design and optimize special heat treatments and predict the resulting microstructures and mechanical properties [1, 2]. These phase transformation curves provide precise information about microstructure resulting from non-isothermal austenite decomposition.

The resulting diagrams serve the needs of the metallurgical industry for further heat treatment of steel. Unfortunately, the availability of CCT diagrams created for transformation of intercritical austenite practically does not exist in open literature and therefore the mechanisms of transformation are not fully understood. Respectively, diagrams can be obtained using various software, but their use is more informative than scientific, since all of these software have to limit their field of activity many times by the percentage limitation of the chemical composition of steels.

2 MATERIALS AND METHODS

The experimental material used in these experiments is high-alloy tool steel X153CrMoV12 used in the engineering industry. It is a high hardenability chromium-vanadium steel suitable for oil and air hardening. Steel is characterized by high wear resistance and is mostly used for cutting tools such as tensioning and extrusion mandrels, profile sheets and complex shaped cutters.

The chemical composition of the experimental samples was verified with a TASMAN Q4 spectrum analyser and is listed in Tab. 1. Its basic mechanical and physical properties are listed in Tab. 2.

Tab. 1 Chemical composition of steel X153CrMoV12 (wt.%)

Element	Min - Max	Spectral analysis
C	1.45-1.60	1.53 ± 0.01
Mn	0.20-0.60	0.21 ± 0.005
Si	0.10-0.40	0.14 ± 0.005
Cr	11.00-13.00	12.25 ± 0.02
Mo	0.70-1.00	0.89 ± 0.01
V	0.70-1.00	0.76 ± 0.01

Source: authors.

Tab. 2 Basic mechanical and physical properties of X153CrMoV12 steel

Mechanical and physical properties	Value
Tensile strength (MPa)	650 - 880
Modulus of elasticity (GPa)	198
Thermal conductivity ($W \cdot m^{-1} \cdot K^{-1}$)	25
Hardness (HV)	790
Specific therm. capacity ($J \cdot kg^{-1} \cdot K^{-1}$)	460

Source: authors.

2.1 Atomic force microscopy

Images were directly obtained using the MFP-3D Infinity AFM microscope (Oxford Instruments). Surface scanning was realized using the AC Air Topography mode, where the cantilever tip is not in constant contact with the tested surface but is vibrates near its resonance frequency and tapes the surface to obtain information of the topography of the tested sample surface. Since this is a relatively high-strength sample, the AC 160TS-R3 cantilever with the spring constant 26 $N.m^{-1}$, resonance frequency 300 Hz and the tip radius in range 5 – 10 nm was used for all performed measurements [3, 4].

3 MICROSTRUCTURE

As is already known, the austenite decomposition and finally formed phases depend on cooling rate. This course of austenite decomposition during continuous cooling corresponds to the discontinuity of the slope detected in the dilatometric curves and is related to the temperature range of specific microstructure type formation. Although the temperature ranges, in which the various phase transformations in the steel can occur, are relatively wide and may even overlap, every phase transformation occurred during the overall continuous cooling process could be detected. The microstructure of the first 10 °C·s^{-1} cooling curve was evaluated as martensitic. Ms temperature was determined as 260 °C. This temperature represents a rate when only the martensitic matrix and the excluded carbides appear in the structure (Fig. 1). In the figure from the AFM microscope, the grain boundaries are clearly visible. In the figure, there are visible small white areas, representing the carbides, and the dark circular areas, representing the holes that have arisen as the carbides ripped from the matrix during grinding process (Fig. 2). Metallographic analysis of the second cooling curve 5 °C·s^{-1} revealed the occurrence of Cr_7C_3 carbides, the martensitic matrix (Fig. 3). As can be seen in the previous figure, the grain boundaries and the primary carbides are clearly visible through the AFM microscope. Only few amounts of bainite have already occurred (Fig. 4). At a third cooling curve of 3 °C·s^{-1}, the incidence ratio of Cr_7C_3 carbides decreased compared to previous cooling rates (Fig. 5, Fig. 6). The matrix was composed of martensite and bainite. At the cooling rate of 1 °C·s^{-1}, a greater amount of bainite than martensite was present in the microstructure. There was still a small amount of Cr_7C_3 chromium carbides in the matrix (Fig. 7, Fig. 8) and the metallographic analysis showed the same occurrence of structures as the expansion of curves. Metallographic analysis shows that at the cooling rate of 0.5 °C·s^{-1}, the morphology of the carbides in the sample was changed to coarse-grained (Fig. 9, Fig. 10). The matrix was predominantly bainite with a low incidence of martensite. In the metallographic analysis (Fig. 11, Fig. 12) in addition to the carbides, about 15 % of pearlite structure was found but was not observed in the dilatation curve. Fe_3C carbides precipitated inside of the matrix grains. The AFM microscope shows a surface topography that confirms the occurrence of a coarse-grained structure. In the last cooling curve, which had the slowest cooling rate of 0.1 °C·s^{-1}, the bainitic and martensitic transformation were connected at the end of the curve, for the martensitic transformation was its limit value. It can be assumed that the device did not notice this change due to a very small change in material volume. In this case, the resulting structure was pearlite with coarsely precipitated Fe_3C carbide according to metallographic analysis (Fig. 13, Fig. 14). Further measurements were not performed because all resulting types of microstructures were achieved.

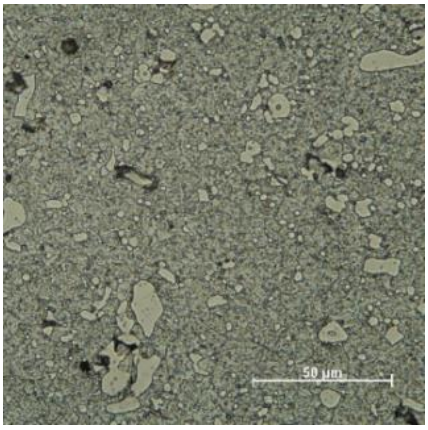

Fig. 1 Microstructure of the cooling curves 10 °C·s^{-1}
Source: authors.

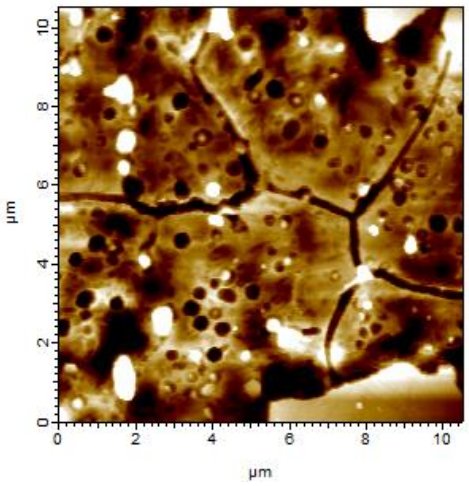

Fig. 2 Surface topography by AFM 10 °C·s^{-1}
Source: authors.

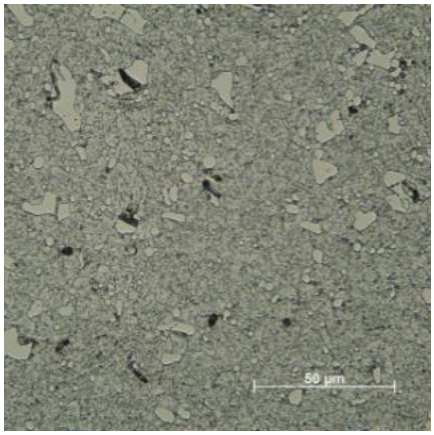

Fig. 3 Microstructure of the cooling curves 5 °C·s^{-1}
Source: authors.

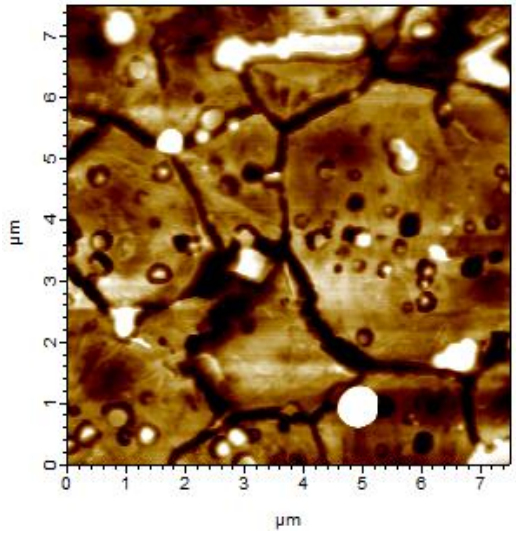

Fig. 4 Surface topography by AFM 5 °C·s^{-1}
Source: authors.

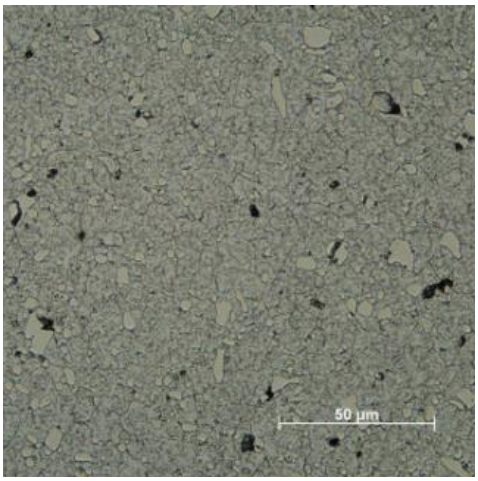

Fig. 5 Microstructure of the cooling curves 3 °C·s^{-1}
Source: authors.

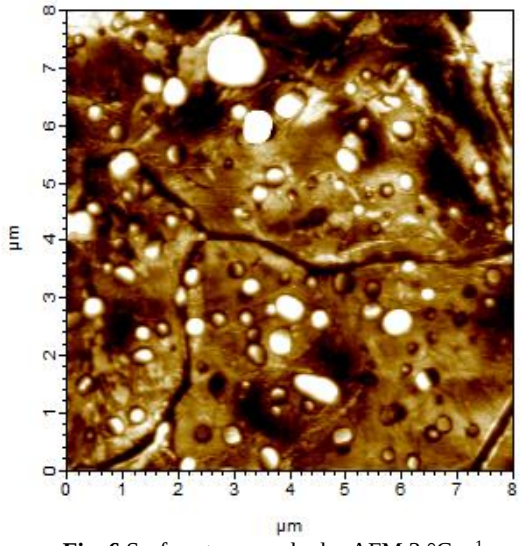

Fig. 6 Surface topography by AFM 3 °C·s^{-1}
Source: authors.

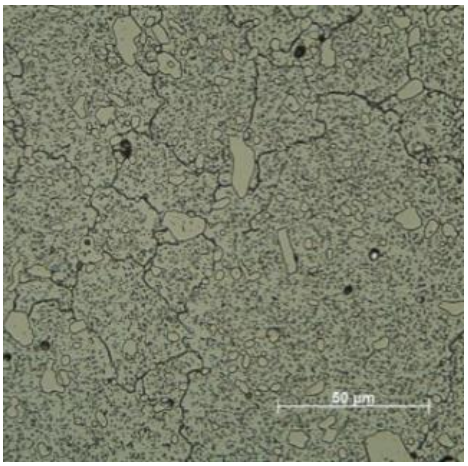

Fig. 7 Surface topography by AFM 1 °C·s^{-1}
Source: authors.

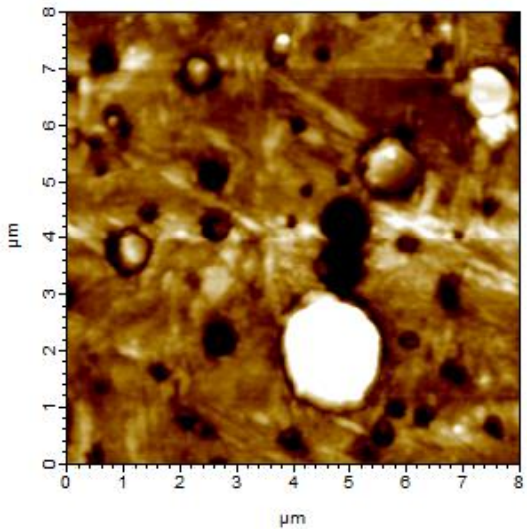

Fig. 8 Surface topography by AFM 1 °C·s^{-1}
Source: authors.

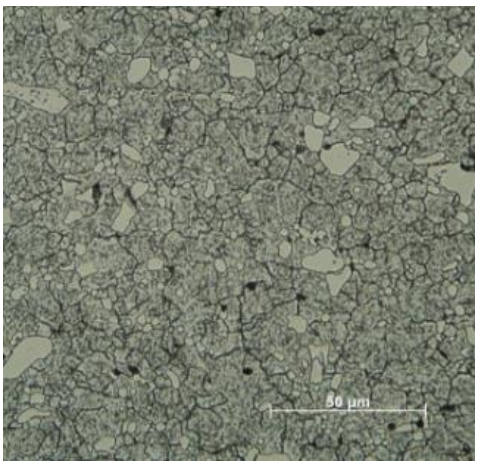

Fig. 9 Surface topography by AFM 0.5 °C·s^{-1}
Source: authors.

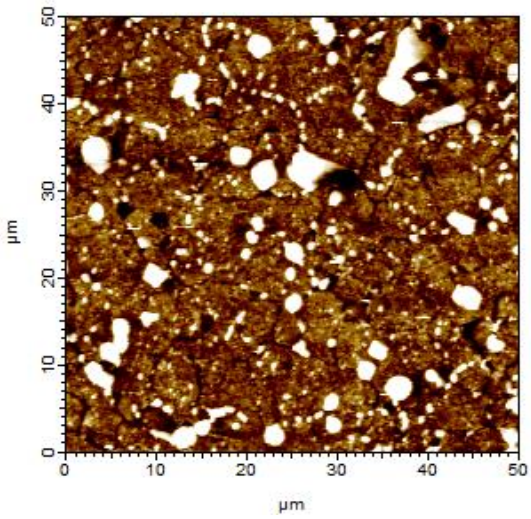

Fig. 10 Surface topography by AFM 0.5 °C·s^{-1}
Source: authors.

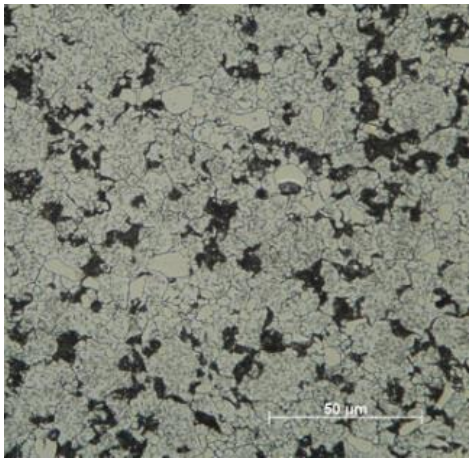

Fig. 11 Surface topography by AFM 0.2 °C·s^{-1}
Source: authors.

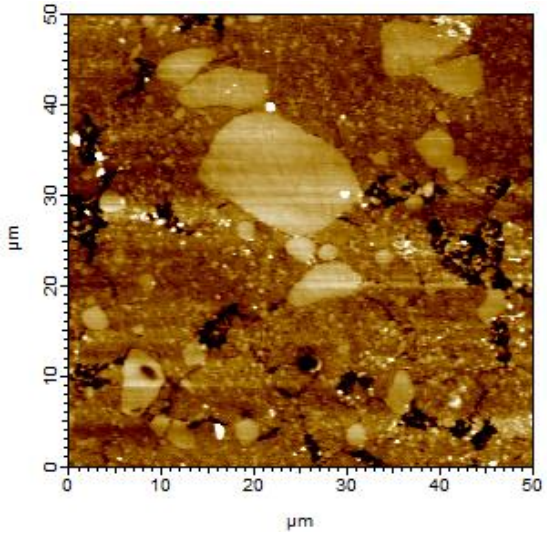

Fig. 12 Surface topography by AFM 0.2 °C·s^{-1}
Source: authors.

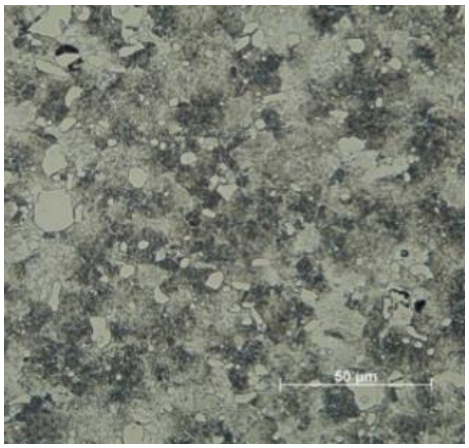

Fig. 13 Surface topography by AFM 0.1 °C·s^{-1}
Source: authors.

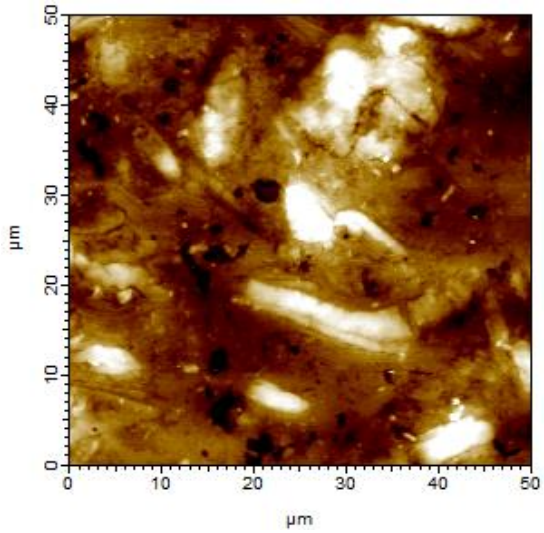

Fig. 14 Surface topography by AFM 0.1 °C·s^{-1}
Source: authors.

4 CCT DIAGRAM OF X153CRMOV12 STEEL

The diagram was constructed from all measured data, i.e. all seven cooling curves. The diagram clearly shows areas of austenite transformation to bainite and martensite. Consequently, at the top we can see the area of pearlitic transformation [5, 6, 7, 8]. Striped red lines mark the temperatures Ac_1 and Ac_3, which point to the transformation of the initial state microstructure to austenite while heating of the sample. A long dark line that extends across all curves points to the formation of carbides in the material. As the cooling rate ended at approximately 100 °C, the martensite finish Mf region was not recorded. At the bottom of each curve, the measured Vickers hardness values are shown at a load of 5 kg. We can notice that the hardness dropped smoothly with the reduction in the cooling rate of the material. The initial temperature was set at 1030 °C on which the time duration was

always 10 min. to continuously overheat the entire sample throughout the bulk of the material. We can notice that second cooling curve (cooling rate of 5 °C·s^{-1}) passes precisely across the boundary that marks the formation of a bainitic change. The critical cooling rate when the pearlite conversion is to be initiated according to the CCT diagram is determined for a cooling rate of approximately 0.15 °C·s^{-1}. Compared to the metallographic structure in the cooling curve of 0.2 °C·s^{-1}, there was not observed any length change due to pearlite formation in the dilatometric curve. This can be due to overlap of the carbide formation and pearlite formation, as each of these processes influence the length change in the opposite direction. The resulting CCT diagram serves as a starting point for the heat treatment of X153CrMoV12 high-strength tool steel (Fig. 15)

.

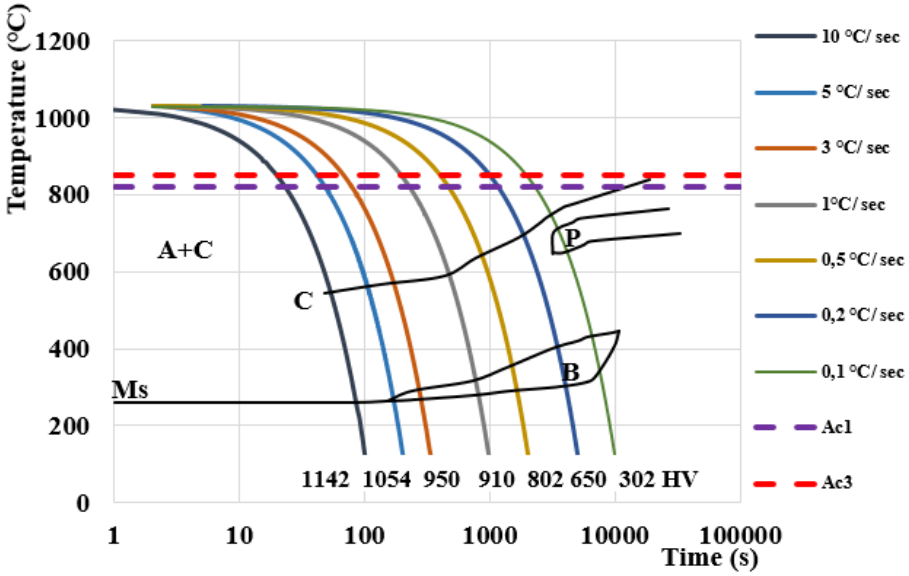

Fig. 15 CCT diagram X153CrMoV12 steel
Source: authors.

5 CONCLUSION

The phase transformation kinetics under continuous cooling conditions was examined in detail using dilatometry, metallographic analysis and nanoindentation hardness test. The results are presented in the form of CCT diagram, which can be useful in designing of the temperature cycles for the production and processing of high performance tool steel X153CrVMo12. The higher percentage of chromium in the material results in the formation of Cr_7C_3 carbide, which results in an increased value of the hardness of the material [9, 10]. Provided the martensitic transformation is achieved, the resulting critical cooling rate is set at 5 °C·s^{-1}. This rate is precisely bordered where literature sources suggests that triple tempering should be followed to achieve the resulting uniform structure of the material. The results of chromium carbides show that at high cooling rates the incidence of hard carbides occur. With decreasing of cooling rates, Fe3C carbides are beginning to occur. Using the AFM microscope, surface topographies of each sample were evaluated to clearly show the sizes of the individual types of carbides as well as their distributions. The resulting sample hardness points to the classic situation where with decreasing cooling rate the hardness of the material decreases and vice versa. The highest hardness achieved value of 1142 HV at the highest cooling rate of 10 °C·s^{-1}. The value of this hardness is mainly affected by the large occurrence of Cr_7C_3 carbides as well as the martensitic matrix.

References

[1] JURČI, P., J. CEJP and J. BRAJER. Metallurgical aspects of laser surface processing of PM Cr-V ledeburitic steel. In: *Advances in Materials, Science and Engineering*. 2011, p. 1-5. ISSN 1687-8434. Available at: https://doi.org/10.1155/2011/563410

[2] PAŠÁK, M., R. ČIČKA, P. BÍLEK, P. JURČI and L. ČAPLOVIČ. Study of phase transformations in Cr-V tool steel. In: *Materiali in Tehnologije*. 2014, **48**(5), p. 693-696. ISSN 1580-2949.

[3] MAN, J., K. OBRTLÍK, C. BLOCHWITZ and J. POLÁK. Atomic force microscopy of surface relief in individual grains of fatigued 316L austenitic stainless steel. In: *Acta Materialia* 2002, **50**(15), p. 3767-3780. ISSN 1359-6454.

Available at: https://doi.org/10.1016/S1359-6454(02)00167-2
[4] MAN, J., B. VALTR, M. WEIDNERC, M. PETRENEC, K. OBRTLÍK and J. POLÁK. AFM study of surface relief evolution in 316L steel fatigued at low and high temperatures. In: *Procedia Engineering*. 2010, **2**(1), p. 1625-1633, ISSN 1877-7058. Available at: https://doi.org/10.1016/j.proeng.2010.03.175
[5] WEI, Y., X. WEI-HONG, L. YA-XIU, B. BING-ZHE and F. HONG-SHENG. Effect of chromium on CCT diagrams of novel air-cooled bainite steels analyzed by neural network. In: *Journal of Iron and Steel Research*. 2007, **14**(4), p. 39-42. ISSN 1006-706X. Available at: https://doi.org/10.1016/S1006-706X(07)60055-7
[6] JIRKOVÁ, H., L. KUČEROVÁ and B. MAŠEK. The Effect of Chromium on Microstructure Development During Q-P Process. In: *Materials today: Proceedings*. 2015, p. 627-630. ISSN 2214-7853. Available at: https://doi.org/10.1016/j.matpr.2015.07.362
[7] SCHINO, A. D. Analysis of phase transformation in high strength low alloyed steels. In: *Metalurgija*. 2017, **54**, p. 349-352. ISSN 0543-5846.
[8] ZRNÍK, J., I. MAMUZIČ and S. V. DOBATKIN. Recent progress in high strength low carbon steels. In: *Metalurgija*. 2006, **45**(4), p. 323-331. ISSN 0543-5846.
[9] KRBAŤA, M., M. ECKERT, D. KRIŽAN, I. BARÉNYI and I. MIKUŠOVA. Hot Deformation process analysis and modelling of X153CrMoV12 steel. In: *Metals*. [online] 2019, **9**(10), p. 1125-1142. Available at: https://doi.org/10.3390/met9101125
[10] BARÉNYI, I., J. MAJERÍK, Z. POKORNÝ and J. SEDLÁK. Material and technological investigation of machined surfaces of the OCHN3MFA steel. In: *Kovové Materiály (Metallic Materials)*. 2019, **57**(2), p. 131-142. ISSN 1338-4252. Available at: https://doi.org/10.4149/km_2019_1_131

Dipl. Eng. Michal **KRBAŤA**, PhD.
Department of Engineering Technologies
and Materials
Faculty of Special Technology
Alexander Dubček University of Trenčín
Ku kyselke 469
911 06 Trenčín
Slovak Republic
E-mail: michal.krbata@tnuni.sk

Dipl. Eng. Róbert **CÍGER**
Department of Engineering Technologies
and Materials
Faculty of Special Technology
Alexander Dubček University of Trenčín
Ku kyselke 469
911 06 Trenčín
Slovak Republic
E-mail: robert.ciger@tnuni.sk

Michal Krbaťa – was born in Trenčín, Slovakia in 1988. He received his Master and PhD. degrees at Alexander Dubček University of Trenčín, Faculty of Special Technology in Trenčín. In his research he focuses on materials research, tribology and dilatometry.

Róbert Cíger – was born in Trenčín, Slovakia in 1996. He received his Master degrees at Alexander Dubček University of Trenčín, Faculty of Special Technology in Trenčín. In his research he focuses on materials research, dilatometry.